Published in final edited form as:
Respir Physiol Neurobiol. 2010 November 30; 174(0): 135–145. doi:10.1016/j.resp.2010.09.006.

Effect of baroreceptor stimulation on the respiratory pattern: Insights into respiratory-sympathetic interactions☆

David M. Baekey[a,*,1], **Yaroslav I. Molkov**[b,1], **Julian F.R. Paton**[c], **Ilya A. Rybak**[b], and **Thomas E. Dick**[a,d]

[a]Department of Medicine, Case Western Reserve University, Cleveland, OH 44106, USA

[b]Department of Neurobiology and Anatomy, Drexel University College of Medicine, Philadelphia, PA 19129, USA

[c]School of Physiology and Pharmacology, Bristol Heart Institute, Medical Sciences Building, University of Bristol, Bristol BS8 1TD, UK

[d]Department of Neurosciences, Case Western Reserve University, Cleveland, OH 44106, USA

Abstract

Sympathetic nerve activity (SNA) is modulated by respiratory activity which indicates the existence of direct interactions between the respiratory and sympathetic networks within the brainstem. Our experimental studies reveal that T_E prolongation evoked by baroreceptor stimulation varies with respiratory phase and depends on the pons. We speculate that the sympathetic baroreceptor reflex, providing negative feedback from baroreceptors to the rostral ventrolateral medulla and SNA, has two pathways: one direct and independent of the respiratory–sympathetic interactions and the other operating via the respiratory pattern generator and is hence dependent on the respiratory modulation of SNA. Our experimental studies in the perfused in situ rat preparation and complementary computational modelling studies support the hypothesis that baroreceptor activation during expiration prolongs the T_E via transient activation of post-inspiratory and inhibition of augmenting expiratory neurones of the Bötzinger Complex (BötC). We propose that these BötC neurones are also involved in the respiratory modulation of SNA, and contribute to the respiratory modulation of the sympathetic baroreceptor reflex.

Keywords

Neural control of respiration; Sympathetic baroreceptor reflex; In situ preparation; Computational modelling

1. Introduction

Cardiac, sympathetic and respiratory activities are coordinated for effective and efficient gas exchange (Hayano et al., 1996). In this regard, the cardiovascular and respiratory systems can be envisioned as an integrated physiological system delivering oxygen to the tissues and

☆This paper is part of a special issue entitled “Central cardiorespiratory regulation: physiology and pathology”, guest-edited by Thomas E. Dick and Paul M. Pilowsky.

*Corresponding author at: Division of Pulmonary, Critical Care and Sleep Medicine, Department of Medicine, Case Western Reserve University School of Medicine, 11000 Euclid Avenue, Room 622 - Mailstop 5067, Cleveland, OH 44106-5067, USA. Tel.: +1 216 368 3964; fax: +1 216 368 0034. david.baekey@case.edu (D.M. Baekey).
[1]These authors contributed equally to this work.

removing carbon dioxide from the body (Koepchen et al., 1981; Richter and Spyer, 1990; Simm et al., 2010). The neural control of this system is located within the brainstem where respiratory rhythm and sympathetic premotor activity are generated. Moreover, the respiratory and sympathetic control circuits interact within the brainstem and various sensory afferents, including baroreceptor inputs, affect the neurones that generate and modulate both respiratory and sympathetic activities.

Sympathetic nerve activity (SNA) expresses respiratory modulation even after vagotomy and decerebration (Barman and Gebber, 1980; Haselton and Guyenet, 1989; Häbler et al., 1994; Richter and Spyer, 1990; Simms et al., 2009) supporting the idea of central coupling between respiratory and sympathetic networks. This coupling seems to be an important mechanism to: (i) optimize minute ventilation and cardiac output to increase the efficiency of oxygen uptake/perfusion at rest; and (ii) allow appropriate dynamic integrative cardiovascular and respiratory reflex responses essential for maintaining homeostasis (Hayano et al., 1996; Zoccal et al., 2009). Therefore, respiratory modulation may contribute to the dynamic control of SNA.

The respiratory rhythm and motor pattern is generated by a respiratory central pattern generator (CPG) located in the lower brainstem (Bianchi et al., 1995; Cohen, 1979; Lumsden, 1923). The pre-Bötzinger Complex (pre-BötC) located within the medullary ventrolateral respiratory column (VRC) is considered a major source of rhythmic inspiratory activity (Feldman and Del Negro, 2006; Koshiya and Smith, 1999; Rekling and Feldman, 1998; Smith et al., 1991). The pre-BötC, interacting with the adjacent Bötzinger Complex (BötC) containing mostly expiratory neurones (Ezure, 1990; Ezure et al., 2003; Jiang and Lipski, 1990; Tian et al., 1999), represents a core of the respiratory CPG (Bianchi et al., 1995; Cohen, 1979; Richter, 1996; Richter and Spyer, 2001; Rybak et al., 2004, 2007, 2008; Smith et al., 2007, 2009; Tian et al., 1999). This core circuitry generates primary respiratory oscillations defined by the intrinsic biophysical properties of respiratory neurones involved, the architecture of network interactions between respiratory neural populations within the pre-BötC and BötC, and inputs from other brainstem compartments, including the pons, retrotrapezoid nucleus (RTN), raphé, and nucleus tractus solitarii (NTS).

The NTS receives and integrates most of the peripheral cardiovascular and respiratory afferent inputs, including baroreceptor afferents. It mediates a variety of reflexive motor responses from the brainstem and spinal cord that provide homeodynamic control of breathing and cardiovascular functions (reviewed by Loewy and Spyer, 1990). The classical baroreflex control of SNA operates via NTS neurones mediating the baroreceptor projections to the caudal ventrolateral medulla (CVLM). Through this path, baroreceptor activation excites CVLM neurones which in turn inhibit the rostral ventrolateral medulla (RVLM) neurones and hence lower SNA (Dampney, 1994; Guyenet, 1990). This pathway provides a direct negative feedback control of SNA.

Respiratory activity is also modulated by the afferent baroreceptor activity possibly through the same NTS baro-sensitive neurones. For instance in vagally intact, decerebrate cats, the activities of approximately 50% of the respiratory-modulated neurones within the VRC responded to transient pressure pulses (Dick and Morris, 2004). Furthermore, expiratory propriobulbar activity was modulated to a greater extent than inspiratory propriobulbar activity (Dick and Morris, 2004). Because the overlap between respiratory and cardiovascular regulatory areas is extensive, we could not exclude the possibility that neurones with both the respiratory-modulated and arterial pulse-modulated activity were related to cardiovascular rather than to respiratory control or to both. To address this, we restricted our analysis to respiratory-modulated activity that was identified as either bulbospinal premotor or bulbar (laryngeal) motor neurones. Surprisingly, these neurones

also exhibited arterial-pulse-pressure modulated activity (Dick et al., 2005).Thus,neurones with an identified respiratory function, modulating airway resistance, can express arterial-pulse modulated activity.

The aim of this study was to verify that activation of baroreceptor afferents can indeed affect the respiratory CPG and the respiratory pattern by altering BötC expiratory neurone firing. We performed systematic recordings of respiratory neurones within the VRC, specifically within the BötC/pre-BötC core of the respiratory network, to reveal possible neural interactions between the baro-afferent processing circuits and those determining the respiratory pattern.

Another important objective of this study was to examine the possibility of parallel pathways for the sympathetic baroreceptor reflex. Parallel pathways, one respiratory modulated and the other independent of respiration has been proposed and identified for the sympathetic chemo-reflex (Guyenet and Koshiya, 1995). The theoretical basis for parallel pathways was derived from the following logic. If respiratory modulation represents an important mechanism for control of SNA and, at the same time, baroreceptor activation can alter the respiratory pattern, then baroreceptor activation should affect SNA via its effects on the respiratory pattern independent of the direct baroreflex pathway from NTS to CVLM. This would provide a basis for suggesting that the sympathetic baroreceptor reflex provides negative feedback from baroreceptors to SNA through two pathways: one direct that is independent of the respiratory–sympathetic interactions, and the other indirect that depends on the effects of baroreceptor afferents on the respiratory pattern and hence on the respiratory modulation of SNA.

Finally, because transection of the pons significantly attenuates respiratory modulation of SNA (Baekey et al., 2008; Dick et al., 2009), we were interested in a possible role of the pons in the baroreceptor reflex mediated respiratory–sympathetic interactions and respiratory modulation of SNA. We used a computational model of the brainstem respiratory network that includes the pons (Smith et al., 2007) and extended it to incorporate VLM, RTN compartments and their corresponding neural populations. The extended model was used to simulate, investigate and predict the possible neural mechanisms involved in the baroreceptor reflex mediated respiratory–sympathetic interactions.

2. Materials and methods

2.1. Surgical and experimental procedures

This series of experiments were performed at two sites: the University of Bristol in Bristol, England, and Case Western Reserve University in Cleveland, OH, USA. For those experiments performed in England, all surgical and experimental procedures conformed to the UK Animals (Scientific Procedures) Act and were approved by the University of Bristol ethical review committee. Similarly, for the experiments done in the United States, the Institutional Animal Care and Use Committee (IACUC) of Case Western Reserve University approved the protocols. The experiments were performed on juvenile (P21–P28, 60–100 g) male rats; these rats were supplied from a Wistar strain at the University of Bristol; whereas those at Case Western Reserve University were Sprague-Dawley.

The rat strain was the only major difference between the two studies because the same individual (David Baekey) performed the experiments using equipment from the same suppliers.

2.2. General surgical methods

We used the arterially perfused *in situ* preparation for these experiments (Paton, 1996). Animals were pretreated with heparin sodium (1000 units – IP), anesthetized with isoflurane (2–3%), and then bisected below the diaphragm. The cranium and thorax were submerged in cold artificial cerebrospinal fluid (aCSF), decerebrated, skinned, and eviscerated. The phrenic nerve and descending aorta were dissected and the dorsal medullary surface exposed.

After this preliminary surgery, the preparation was mounted supine in a stereotaxic frame in the recording chamber. The descending aorta was cannulated with a #4 French, double-lumen catheter (Braintree Scientific).Through one lumen, the preparation was perfused with iso-osmotic aCSF saturated with 95% O2/5% CO2 (21–28ml/min, Marlow Watson 505S peristaltic pump). Through the other lumen perfusion pressure was monitored (CWE TA-100 transducer-amplifier). Perfusion pressure was maintained at 60–80 mm Hg and supported with 4 μM vasopressin (20 μl added to perfusate, basically to restore the vasopressin lost by removing the blood and hypothalamus). The preparation was immobilized with vecuronium bromide (0.4 mg/200 ml perfusate). Sodium cyanide (0.1%, 50 ul-bolus intra-arterial) was used to initiate rhythmic respiratory activity through robust, transient stimulation of the carotid chemoreceptors.

2.3. Ponto-medullary transection

The left phrenic nerve and thoracic sympathetic nerves were drawn into suction electrodes and efferent neural activities were amplified (Grass P511), filtered (0.1–3 KHz) and digitized using a CED Power 1401 connected to a Dell Personal Computer running CED Spike2 software.

After placement of the peripheral nerves in the recording electrodes and baseline recordings including the characterizing the responses to transient increases in the perfusion pressure to stimulate arterial baroreceptors, the pons was separated from the medulla (Baekey et al., 2008). Briefly, a razor blade trimmed to the appropriate width was lowered perpendicularly through the brainstem approximately 3 mm rostral to calamus scriptorius (Baekey et al., 2008). This transection resulted in a transient suppression of respiratory efferents followed by an unstable apneustic pattern. If the respiratory rhythm needed to be restored, the percent of carbon dioxide was increased in the aCSF for the duration of the recording.

After the post-transection baseline recording, perfusion pressure of the preparation was transiently increased for comparison with the “intact” state (Fig. 1B).

2.4. Electrode placement and neuronal sampling strategy

The multi-electrode array was secured to a stereotaxic frame allowing the 16 tungsten microelectrodes (10–12 MΩ.) to be aligned perpendicularly to the dorsal medullary surface. Eight electrodes were on either side of the brainstem in two rows of four electrodes oriented sagittally. The two rows were separated 250 μm while electrodes within each row were separated by 300 μm. Stereotaxic coordinates were used to position electrodes bilaterally in the rostral lateral medulla. The depth of each electrode was positioned in steps as small as a micron and this adjustment was used to maximize signal-to-noise ratio and to isolate the recording of activity to a single source. In cases where more than one neurone was recorded on a single electrode, the principle component analysis (PCA) feature of the Spike2 software was used to discriminate individual spike trains (spike sorting). The independent depth adjustment of each electrode optimized the yield of parallel single neurone recordings.

2.5. Data analysis

The recorded data include: phrenic nerve activity (PNA), thoracic sympathetic nerve activity (tSNA) and extracellular potentials from the microelectrode array. PNA was processed by removal of any DC offset, rectification and smoothing using a 100-ms time constant to obtain a moving-time average of activity. From this 'integrated' PNA, we marked the onsets of inspiratory and expiratory phases. Action potentials of single neurones were converted to times of occurrence, i.e. spike trains (Fig. 5B).

The following measures were computed from a 10-min baseline period in order to ensure that there was only one neurone per channel and to characterize the cell-type: (1) Autocorrelation histograms were created for each spike train to ensure that it represents the activity of a single neurone (not shown). A spike train with potentials from two or more neurones would include short intervals not constrained by refractoriness. (2) Cycle-triggered histograms were used to classify activity patterns with significant respiratory modulation according to the phase (inspiratory or expiratory) in which they are more active and by trends in their burst patterns (augmenting, decrementing or plateau). (3) The firing rate histograms were plotted (Fig. 5B – 100ms bins) to examine the influence of arterial pulse pressures on activity.

2.6. Modelling and simulations

The model was developed based on, and as an extension of, the previous model described by Smith et al. (2007). All neurones were modelled in the Hodgkin–Huxley style (single-compartment models) and incorporated known biophysical properties and channel kinetics characterized in respiratory neurones *in vitro*. Each neuronal type was represented by a population of 20–50 neurones. Heterogeneity of neurones within each population was set by a random distribution of some parameters and the initial conditions for values of membrane potential, calcium concentrations, and channel conductances. A full description of the previous model and model parameters can be found in Smith et al. (2007). All new (additional) and altered (relative to Smith et al, 2007) model parameters are indicated in Table 1 in the Appendix.

All simulations were performed with a simulation package NSM 3.0. developed at Drexel University by S.N. Markin, I.A. Rybak, and N.A. Shevtsova. Differential equations were solved using the exponential Euler integration method with a step of 0.1 ms. Other details of modelling and simulation methods can be found in Smith et al. (2007).

3. Results

3.1. Respiratory phase-dependent and pontine-dependent effects of transient baroreceptor stimulation on the respiratory pattern and on respiratory modulation of sympathetic nerve activity

In the intact arterially perfused in situ rat preparation, the thoracic sympathetic nerve activity (tSNA) usually exhibited a well-expressed positive inspiratory modulation reaching its peak in early post-inspiration (see Fig. 1A1–A3 before applied stimulations). The respiratory modulation of tSNA was significantly suppressed or eliminated after removal of the pons when phrenic nerve activity (PNA) transformed to a more apneustic-like pattern with prolonged inspiratory bursts and shortened expiration periods (see Fig. 1B before applied stimulation) hence confirming a critical role of the pons for the observed respiratory modulation of tSNA as reported previously (Baekey et al., 2008).

The transient increases in the perfusion pressure (PP) were induced by increases in flow of perfusate with the amplitude slightly above the threshold for evoking the sympathetic

baroreflex (Baekey et al., 2008; Dick et al., 2009; Simms et al., 2007). These stimuli were delivered during inspiration, post-inspiration or late expiration and produced an obvious respiratory phase-dependent effect on the respiratory pattern (evaluated by phrenic nerve activity, PNA) and, correspondingly, on the respiratory modulation of tSNA (Fig. 1A1–A3).

With pons intact, the barostimulation had almost no effect on the amplitude and duration (i.e. inspiratory period, T_I) of the phrenic bursts even when stimuli were delivered during inspiration (Fig. 1A1, n=8 animals). At the same time, these stimuli suppressed or abolished respiratory modulation of tSNA. The baroreflex in all these cases persisted, i.e. tSNA was suppressed during barostimulation. In contrast, the same stimuli applied during post-inspiration and late expiration produced an increase in the expiration period (T_E) and decrease in tSNA. The barostimulation-evoked prolongation of T_E was greater if stimulation was applied later during the expiratory phase. For example, Fig. 1A2 and A3 shows a greater increase in T_E when stimulation was delivered later in expiration (panel A3), than when it was applied during post-inspiration (panel A2).

As mentioned above and previously (Baekey et al., 2008; Dick et al., 2009), after pontine transection the respiratory modulation of tSNA was greatly reduced. However, the baroreflex persisted (lowering tSNA during baroreceptor stimulation). Further, when the perfusion pressure pulse was applied during the prolonged inspiration, the barostimulation shortened the apneustic burst (Fig. 1B), which is stark contrast to a negligible effect on T_I in the intact state (Fig. 1A1).

3.2. Conceptual model and hypotheses

Fig. 2 represents our conceptual schematic of respiratory– sympathetic interactions in the context of the sympathetic baroreceptor reflex. The schematic is based in part on our experimental studies described above and previously (Baekey et al., 2008; Dick et al., 2009), as well as on various data in the literature. Specifically, we hypothesize that sympathetic baroreflex operates via two pathways (see solid black arrows in Fig. 2). The first path leads from NTS to the CVLM, which in turn inhibits RVLM neurones hence lowering sympathetic motor output (Dampney, 1994; Guyenet, 1990). This pathway avoids respiratory circuits and provides negative feedback control of SNA independent of the respiratory activity.

The second pathway is mediated by respiratory circuits in the VRC and pons and represents a baroreflex component dependent on the respiratory–sympathetic interactions. As mentioned above, the respiratory modulation of sympathetic activity includes inspiratory activation and post-inspiratory inhibition or disfacilitation (Fig. 1A1–A3). Because both these modulatory influences require the pons to be intact for their expression (Fig. 1B), and because baroreceptor stimulation in the intact preparation prolongs expiration (Fig. 1A2 and A3), we hypothesize that the respiratory modulation of SNA is mainly provided by two types of connections to the RVLM (grey arrows in Fig. 2): (1) a direct excitatory connection from pontine neurones whose activity increases during inspiration peaking during the inspiratory-to-expiratory phase transition (IE neurones), providing the positive inspiratory and IE phase transition modulation of RVLM neurones and SNA; and (2) inhibitory connections from the post-inspiratory neurones of the VRC, whose activity critically depends on pontine drive (Dutschmann and Herbert, 2006; Rybak et al., 2004; Smith et al., 2007) and is controlled by inputs from baroresponsive RTN neurones (see above). The latter connections provide the negative post-inspiratory modulation of RVLM neurones and SNA. Therefore, we specifically hypothesize that (with pons intact) the second baroreflex pathway operates via the activation of VRC's post-I neurones (Fig. 2) that prolong expiration and inhibit RVLM neurones and SNA (Fig. 1A2 and A3).

The respiratory modulation of pontine neurones, including inspiratory and phase-spanning inspiratory–expiratory types, is provided by various projections of VRC's respiratory neurones to the corresponding pontine neurones (indicated by the grey arrow from VRC to pons in Fig. 2; see Ezure and Tanaka, 2006; Rybak et al., 2004, 2008; Segers et al., 2008).

Our experimental data (Fig. 1A1) also suggest that when the pons is intact the effect of baroreceptor stimulation on the respiratory rhythm is minimal during inspiration implying that the NTS barosensitive interneurones that excite post-I neurones of VRC are suppressed during inspiratory phase. In contrast, shortening of the inspiratory (PNA) bursts by baroreceptor stimulation is observed after pontine removal (Fig. 1B). Hence, we hypothesize the existence of inspiratory inhibition (gain reduction) of the barosensitive NTS neurones during inspiration (dashed arrows in Fig. 2), which can potentially be produced by either pontine (inspiratory modulated) neurones (Felder and Mifflin, 1988; Potter, 1981), or inhibitory inspiratory neurones of VRC (e.g. see Miyazaki et al., 1999), whose activity depends on pontine drive.

3.3. Computational modelling

One of the objectives of this study was to investigate the above conceptual model and hypotheses proposed using computational modelling. We used the previously published large-scale computational model of the brainstem respiratory network (Smith et al., 2007) and extended this model by incorporating NTS, RVLM, CVLM and lateral pontine compartments (see Fig. 3). The basic model described interactions among respiratory neurone populations spatially organized within the lateral brainstem, extending from the pons to the lower medulla. Similar to that model, the respiratory brainstem populations in the extended model (see Fig. 3) include (right-to-left): a ramp-inspiratory (ramp-I) population of premotor bulbospinal inspiratory neurones and an inhibitory early-inspiratory (early-I(2)) population located in the rostral ventral respiratory group (rVRG); a pre-inspiratory/inspiratory (pre-I/I) and an inhibitory early-inspiratory (early-I(1)) populations of the pre-Bötzinger Complex (pre-BötC), and an inhibitory augmenting-expiratory (aug-E) and a post-inspiratory (post-I) populations and an excitatory pre-motor post-I(e) populations in the Bötzinger Complex (BötC). The BötC's and pre-BötC's populations together represent a core circuitry of the respiratory CPG (Rybak et al., 2007; Smith et al., 2007). In addition, multiple drives from other brainstem components, including the pons, RTN, and raphé pro-vide excitatory drives that regulate the dynamic behaviour of this core circuitry, as well as the activity of premotor neurone populations in the rVRG and phrenic motor output (PN) [note to distinguish the model's data from the experimental recordings we have purposefully introduce new abbreviations to PN rather than PNA and SN rather than tSNA]. The respiratory oscillations in the model emerge within the BötC/pre-BötC core circuitry due to dynamic interactions between (i) the excitatory neural population in pre-BötC active during inspiration (pre-I/I), (ii) the inhibitory population in pre-BötC that provides inspiratory inhibition within the network (early-I(1)); and (iii) the inhibitory populations in the BötC generating expiratory inhibition (post-I and aug-E) (see Rybak et al., 2007; Smith et al., 2007).

To extend this model, we have incorporated the following new neural populations (see Fig. 3): (1) RVLM and CVLM populations comprising the ventrolateral medulla (VLM) compartment; (2) a pontine IE neural population; and (3) two identical neural populations of second-order barosensitive cells in the NTS. Similar to other populations in the model, each of these populations contains 20–50 neurones with randomized parameters modelled in the Hodgkin–Huxley style (single-compartment models). The neurones in these populations contain only a minimal set of ion channels necessary for spike generation (fast sodium, potassium rectifier and leakage) with the same parameters as those used for other neurones of this type in the basic model (e.g., ramp-I neurones, see Smith et al., 2007).

The RVLM and CVLM populations were added as these compartments are considered critical for sympathetic output (Dampney, 1994; Guyenet, 2000). Neurones with phase-spanning IE pattern and the peak of the activity at the end of inspiration have been found in the rostral pons (Cohen and Wang, 1959; Dick et al., 1994, 2008; Segers et al., 2008; Takagi and Nakayama, 1958). The two populations of barosensitive neurones in the NTS receive "barostimulation" in our simulations. The applied stimuli were simulated as excitatory synaptic drive to these populations with time-dependent function reproducing the dynamics of PP in the corresponding experiments (see bottom traces in Figs. 4 and 5A).

The following connections between the incorporated populations described above and other neural populations have been included in the model (Fig. 3; see also Table 1 in the Appendix):

1. Excitatory connections from the RVLM population to the sympathetic preganglionic neurones (IML), which define the sympathetic motor output (SNA; Dampney, 1994; Guyenet, 2000).
2. Inhibitory connections from the CVLM to the RVLM population and excitatory connections from the population of second-order barosensitive neurones in NTS to the inhibitory CVLM population which represent the classical, direct pathway of sympathetic baroreflex (Guyenet, 2000; Mandel and Schreihofer, 2006, 2009).
3. Excitatory connections from the ramp-I population of rVRG and from post-I(e) population in BötC to the pontine IE population which are proposed to form the phase-spanning IE pattern of the latter (see Rybak et al., 2004);
4. Excitatory connections from the pontine IE population to the RVLM population, which we specifically hypothesize in this study to provide the pontine-dependent inspiratory and post-inspiratory modulation of SNA (see Fig. 1A1–A3).
5. Inhibitory connections from the post-I population of BötC to the RVLM population, which we hypothesize to explain the negative post-inspiratory modulation of SNA (Fig. 1A1–A3). The latter modulation is pontine-dependent, since in our model pontine drive is necessary for the expression of post-I activity (see Rybak et al., 2007; Smith et al., 2007). Note that direct connections from the BötC region to RVLM have been previously experimentally identified by Sun et al. (1997).
6. Excitatory connections from one population of second-order barosensitive neurones in the NTS to the post-I population of BötC, which is hypothetically responsible for the prolongation of expiration during baroreceptor stimulation (Fig. 1A2 and A3).
7. Finally, we put a hypothetical inhibitory connection from the pontine-dependent early-I(2) population of rVRG to the second-order barosensitive NTS population projecting to the post-I neurones to control (reduce) the gain of barostimulation on the respiratory pattern during inspiration. This central control of NTS cells during inspiration has been demonstrated for the NTS pump cells by Miyazaki et al. (1999) and P cells do receive baro-receptor input (Rogers et al., 1993). This central control of baroreflex gain in the model is pontine-dependent, since in our model pontine drive is necessary for the expression of activity in the early-I(2) population (see Rybak et al., 2007; Smith et al., 2007).

Fig. 4 shows the results of our simulation of the effects of transient barostimulation during different phases of the respiratory cycle using the "intact" model (Fig. 4A1–A3) and after removal of the pontine compartment (Fig. 4B). Under normal conditions (i.e. with pons intact and in the absence of "baroreceptor stimulation") the model generates a three-phase eupnoea-like respiratory pattern and augmenting PN bursts similar to those observed in the

in situ preparations under normal conditions (see PN output in Fig. 4A1–A3, all details can be found in Smith et al., 2007). Similar to our experimental records (Fig. 1A1–A3), the sympathetic output (SN) in the model exhibits a positive inspiratory and post-inspiratory modulation provided by the pontine IE population to RVLM and a rapid-offset during post-inspiratory resulting from the inhibitory inputs from the post-I population of BötC to the RVLM (see Figs. 3 and 4A1–A3). Transient barostimulation applied to the barosensitive NTS populations produces a temporal reduction of sympathetic output via direct activation of the CVLM population that inhibits the activity of RVLM population. This represents the direct, respiratory-independent component of the sympathetic baroreflex.

Baroreceptor stimulus application during inspiration does not affect respiratory (PN) activity in the model because the gain of the input from the barosensitive NTS population to the post-I neurones is suppressed centrally during inspiration by the inhibitory early-I(2) population of rVRG (see Fig. 4A1 and compare with Fig. 1A1). In contrast, stimuli applied during late expiration (Fig. 4A3) prolong expiration via activation of post-I neurones of BötC, which inhibit the aug-E population and the RVLM. These interactions represent a second component of the sympathetic baroreflex involving interactions between the respiratory and sympathetic circuits. Note that, similar to our experimental data (Fig. 1A3), stimulation-evoked prolongation of expiration is greater if stimulation is applied later during the expiratory phase (Fig. 4A2 and A3).

Removing the pontine compartment in the model converts the normal eupnoea-like respiratory pattern to the apneustic pattern characterized by prolonged PN busts with a rectangle-like profile (see Fig. 4B). As shown previously (Rybak et al., 2007; Smith et al., 2007), this pattern is characterized by a lack of post-I activity that is strongly dependent on pontine drive. With the removal of the pons in the model, the respiratory modulation of SNA (formed by inputs from the IE pontine population and the BötC's post-I population to RVLM) is abolished (see Fig. 4B and compare with Fig. 1B). Simultaneously, the central suppression of the baroreflex gain by the rVRG's early-I(2) population, whose activity in the model is also dependent on the pontine drive, is eliminated with the pontine removal. Therefore the applied "barostimulation" can activate post-I population during inspiration and produce an advanced termination of the apneustic inspiratory bursts hence shortening inspiration (see Fig. 4B and compare with Fig. 1B).

Fig. 5A illustrates the neural mechanism by which the transient barostimulation applied during expiration prolongs this expiration in the intact model. This simulation corresponds to the case shown in Fig. 4A3. The post-I neurones of BötC when activated inhibit all inspiratory (and aug-E) neurones and initiate the post-inspiratory phase of expiration. During expiration these neurones adapt hence releasing activity of the aug-E neurones from inhibition allowing for their gradual activation (see unperturbed breathing cycles in Fig. 5A). When a barostimulus comes during expiration, the post-I population is activated again and inhibits the aug-E population, hence producing a "resetting of expiration". The aug-E population then is activated second time. This resetting of expiration by the transient barostimulation applied during expiration results in the observed prolongation of expiration duration.

3.4. Transient pressure pulses delivered during expiration prolong this expiration via activation of post-I neurones of the Bötzinger Complex in situ

Given the consistent prolongation of T_E in response to transient pressure pulses (see Fig. 1A2 and A3) and our modelling predictions (Fig. 5A), we investigated the responses of expiratory neurones of BötC to baroreceptor stimulation. Preliminary experiments (n=4 animals) were performed using the arterially perfused in situ preparations of juvenile rats. Extracellular recordings were made from neurones within the region extending 1.7–2.7mm

rostral to the obex, from 1.2 to 2.2mm lateral to the midline, and ventrally ~2.6mm below the dorsal medullary surface. This area corresponded to the BötC in the rat (Paxinos and Watson, 1998.). We focused on determining the response to barostimulation on expiratory decrementing (post-I) and expiratory augmenting (aug-E) neurones (see example in Fig. 5B). We recorded decrementing (post-I type (n=7) and augmenting expiratory neurones with the latter augmenting throughout the phase (aug-E type, n=6). When perfusion pressure was increased transiently, the activity of post-I neurones increased (n=5 of 7) and the activity of aug-E neurones decreased (n=6 of 6) in full accordance with the model prediction (see example shown in Fig. 5B and compare with Fig. 5A). This pattern of activation/deactivation of post-I and aug-E cells, respectively, was consistent with the reciprocal inhibitory connections between the post-I and aug-E neurones in the BötC (see Fig. 3). In the majority of cases (n= 15 of 25), the barostimulation applied during expiration resulted in the prolongation of T_E, and this prolongation was greater when stimulation was applied later in expiration.

4. Discussion

4.1. Respiratory modulation of sympathetic activity

In this study, we focus on two aspects of the respiratory modulation of SNA: the positive inspiratory (or IE with the peak during early post-inspiration) and the subsequent post-inspiration rapid off-set that can be recognized in our experimental recordings in situ (Fig. 1A1–A3). Our data support the anatomical evidence that sympatho-respiratory coupling occurs, at least partially, in the medulla (Pilowsky et al., 1990, 1992, 1994; Sun et al., 1997). However, recordings from RVLM and CVLM neurones have revealed more complex respiratory-modulated activity patterns supporting broader interactions between the brainstem respiratory neurones and neurones within RVLM and CVLM than we have developed here. For example, Mandel and Schreihofer (2006) revealed at least four distinct respiratory modulated discharge patterns: inspiratory modulated activity with a peak during PNA; expiratory modulated activity decreasing during PNA; expiratory–inspiratory modulated activity, and post-inspiratory modulated activity. These four types of respiratory-modulated activity were established using cycle-triggered histograms of neuronal activity correlated to cycle triggered averages of integrated phrenic nerve activity (PNA). With our initial model, we have reproduced aspects of the respiratory-modulated SNA pattern without all the respiratory-modulated activities expressed in RVLM/CVLM. This issue requires further development of the model.

While our model does not contain connections between the respiratory pattern generator and neurones in CVLM, it replicates major features of sympatho-respiratory patterning. Additional experimental data are needed to elaborate, validate or revise the model. Specifically, another possibility is that the respiratory modulation of RVLM neurones is related through CVLM.

According to our previous (Baekey et al., 2008; Dick et al., 2009)and current studies,the magnitude of respiratory modulation of SNA depends on the pons being intact (Fig. 1B). After ponto-medullary transection, respiratory modulation is only weakly seen in thoracic sympathetic nerve activity. This reduced coupling of phrenic and sympathetic nerve activities following ponto-medullary transection is similar to that of the decerebrate rat after systemic administration of MK-801, an NMDA antagonist (Morrison, 1996). Further, the effects of MK-801 on the respiratory pattern (decreased amplitude, apneusis, increased variability) mirror those of ponto-medullary transection (Lumsden, 1923; Smith et al., 2007). The significant reduction of SNA respiratory modulation with removal or suppression of the pons suggests that RVLM/CVLM neurones defining the SNA profile either receive direct projections from respiratory modulated pontine neurones or receive

inputs from the respiratory neurones in VRC whose activity critically depends on pontine input. Thus, the respiratory modulation of SNA could be mediated directly by pontine IE neurones and/or indirectly by BötC's post-I neurones, whose activity was, in part, pontine-dependent. This scenario was implemented in our model. Other possible solutions will be comparatively considered in our future studies.

4.2. Effects of baroreceptor stimulation on the respiratory pattern and the activity of respiratory neurones

Our data provide a neural substrate for the expiratory– facilitatory response to activation of baroreceptors (Brunner et al., 1982; Dove and Katona, 1985; Grunstein et al., 1975; Li et al., 1999a,b; Lindsey et al., 1998; Nishino and Honda, 1982; Richter and Seller, 1975; Speck and Webber, 1983; Stella et al., 2001). We clearly demonstrate that barostimulation activates post-I neurones and depresses aug-E neurones. This is consistent with our previous finding that respiratory neurones, preferentially expiratory neurones, are modulated with the arterial pulse (Dick and Morris, 2004; Dick et al., 2005). In contrast, these findings differ from those of Kanjhan et al. (1995) who did not find barosensitive neurones in the BötC and to McMullan et al. (2009) who found only a modest increase in T_E evoked by aortic depressor nerve (ADN) stimulation.

Our model replicates prolongation of expiration and identifies possible network interactions following baroreceptor activation.

The prolongation of expiration in response to abrupt increases in blood pressure does not appear to have a teleological explanation. On the other hand the inverse, volitional slowing of breathing or Pranayamic breathing is a recognized practice that decreases blood pressure. The mechanism is unclear but prolonged expiration may increase vagal tone (to decrease heart rate) and decrease venous return (temporary cessation of abdominal thoracic pumping), vascular resistance and cardiac work.

A prolongation of expiratory period through activation of post-I neurones also occurs in the diving response (Dutschmann and Paton, 2002). This evokes an increase in cardiac vagal tone (bradycardia), systemic vasoconstriction as well as an apnoea (Daly, 1984, 1986; Elsner et al., 1966a,b; Whayne and Killip, 1967). The respiratory-sympathetic coupling present in the diving response is strong enough to reverse paroxysmal supraventricular tachycardia (Bisset et al., 1980; Wildenthal et al., 1975).

In the experiments of McMullan et al. (2009), only a 30% increase in T_E was associated with ADN stimulation. The experiments of McMullan et al. (2009) were performed in an anesthetized rat whereas in our studies the rats were decerebrate. The difference between stimuli may also be afactor in the different results. We delivered a pressure pulse directly to the arterial system that affected all of the baroreceptors, In contrast, McMullan et al., tested a T_E baroresponse by pharmacologic agents (phenylepherine and Angiotension II) as well as by ADN stimulation and definitely did not observe a robust prolongation of expiration. As discussed later the role of anesthetics may be critical in evoking the response of a prolongation in T_E.

Expiratory brainstem activity sensitive to baroreceptor has not been found in anesthetized rats (Kanjhan et al., 1995) but has been reported in anesthetized (Lindsey et al., 1998) and decerebrate (Dick and Morris, 2004; Dick et al., 2005) cats. In pentobarbital-anaesthetized rats, BötC neurones were recorded and identified on the basis of location, phasic expiratory activity, and proprio-bulbar axons. None (n=29) of the recorded neurones had systole-triggered histograms with a feature indicating sensitivity to baroreceptor input nor a response to a baro-stimulus that consisted of three current pulses delivered to ADN

(Kanjhan et al., 1995). Contrasting this in Dial-urethane anaesthetized cats, six of seven ventrolateral medullary post-I neurones increased their firing rate during baroreceptor stimulation and their increases were associated with T_E prolongation. Similarly in decerebrate cats, nearly half (96/200) of the respiratory modulated neurones had arterial-pulse modulated activity (Dick and Morris, 2004). In this and a subsequent study (Dick et al., 2005), expiratory activity was preferentially modulated with arterial pulse pressure.

The obvious differences in these studies were anesthetic and species, however, these are unsatisfying explanations. Another possibility may be related to an observation we made in that pulse-modulated activity was grouped in certain ensemble recordings in which the animal had a high pulse pressure. Thus, the magnitude and prevalence of pulse-modulated activity may be a function of the magnitude of the pulse pressure. Indeed, the percentage of simultaneously recorded neurones exhibiting pulse-modulated activity was significantly correlated with pulse pressure (Dick and Morris, 2004). Despite this correlation the raw records from Kanjhan et al. have a robust (appearing to range from 30 to 50mmHg) arterial pulse pressure whereas the perfused rat has a minimal pulse pressure (but the transient increases in perfusion pressure are approximately 60mmHg thereby mimicking large pressure pulses). In summary we have a plausible explanation as to why Kanjhan et al. (1995) did not find baromodulated activity in Bötzinger Complex activity in rats.

4.3. Computational model

Our model represents a first attempt to integrate sympatho-respiratory circuits. The model clarifies the role of baroreceptors in activating post-I neurones and thereby indirectly inhibiting aug-E neurones and demonstrates that excitatory synaptic drive to the post-I neurones can account for the prolongation in expiration.

The model focuses on the interaction between BötC and RVLM. The primary cell types in the BötC are inhibitory although excitatory post-I neurones may exist and may be responsible for post-I modu-latory projections to the pons and for upper airway motor control. Therefore, future modelling could be based on VRC interaction with the RVLM/CVLM using both inhibitory and excitatory connections. For example, should excitatory post-I neurones project to the CVLM and in turn these CVLM neurones inhibit RVLM activity, this would produce the same result as the current model shows. Also, as mentioned above, our current model does not account for the different respiratory-modulated patterns observed in CVLM neurones (Mandel and Schreihofer, 2006).Clarification of the respiratory network interactions with the RVLM and CVLM will be in focus of our future modelling studies.

Post-I neurones in our model display a reduction in the rate of decline in firing frequency, and prolongation of their discharge that provides an increase in expiratory duration (Feldman and Cohen, 1978; Hayashi et al., 1996; Krolo et al., 2005; Manabe and Ezure, 1988; Parkes et al., 1994). Our model contains a special population of baro-sensitive cells in the NTS projecting to the post-I neurones, whose activity is controlled centrally (in the current model by early-I(2) population of rVRG). This population could be P-cells as they are activated in the baroreflex (Rogers et al., 1993). Interestingly, the model is consistent with the control of the NTS pump (P) cells receiving early-inspiratory inhibition previously described by Miyazaki et al. (1999). Because stimulation of pulmonary afferents activates post-I neurones via P cells of NTS (Hayashi et al., 1996), P cells may be involved in both the Hering–Breuer reflex and baro-respiratory response. Yet another possibility for control of the gain of baroreflex at the level of NTS could be if early inspiratory inhibition comes from the pons (see Fig. 2). Indeed, electrical stimulation of parabrachial nucleus suppresses the gain of carotid sinus afferent input to NTS (Felder and Mifflin, 1988), so the control of baroreflex gain can be modelled by incorporating inhibitory inspiratory population to the

pontine compartment projecting to the second-order baro-sensitive cells in the NTS that excite post-I neurones.

4.4. Two pathways of the sympathetic baroreceptor reflex in the brainstem

The results of our experimental and modelling studies support the proposed concept (Fig. 2) that the sympathetic baroreceptor reflex, providing negative feedback from baroreceptors to the rostral ventrolateral medulla and SNA, has two pathways. The first, direct path leads from the baroreceptor neurones in NTS to CVLM which inhibits RVLM hence lowering SNA (Dampney, 1994; Guyenet, 1990). The second pathway is mediated by respiratory circuits, specifically by the post-I neurones of BötC which inhibit RVLM and prolong expiration. This baroreflex pathway is strongly dependent on the respiratory–sympathetic interactions and requires an intact pons to be expressed. This concept, similar to that developed by Guyenet and Koshiya for the sympathetic chemoreflex (Guyenet, 2000; Guyenet and Koshiya, 1995; Koshiya and Guyenet, 1996) requires further experimental investigations.

Acknowledgments

We gratefully acknowledge the support of NIH grants R33 HL087377, NS057815, HL090554, and HL033610; American Heart Association, SDG 073503N; and the British Heart Foundation. David Baekey was also funded by a Leverhulme Fellowship from the University of Bristol. J.F.R.P. was in receipt of a Royal Society Wolfsom Research Merit Award.

Appendix A

See Table A.1.

Table A1

Weights of synaptic connections in the network.

Target population (location)	Excitatory drive {weight of synaptic input} or source population {weight of synaptic input from single neuron}
ramp-I (rVRG)	drive(pons) {2.0}; early-I(2) {−0.3} *; pre-I/I{0.06}; aug-E{−0.1} *; post-I {−2.0} *.
early-I(2) (rVRG)	drive(pons) {2.5} *; aug-E {−0.25}; post-I {−0.5} *.
pre-I/I (pre-BötC)	drive(raphe) {0.3}; drive(RTN) {0.22} *; drive(pons) {0.65} *; pre-I/I {0.03}; aug-E {−0.06} *; post-I {−0.16} *.
early-I(1) (pre-BötC)	drive(RTN) {1} *; drive(pons) {1.1}; pre-I/I {0.1}; * aug-E {−0.265} *; post-I {−0.45} *.
aug-E (BötC)	drive(RTN) {1.5} *; drive(pons) {1.2} *; early-I(1) {−0.135} *; post-I {−-0.3}.
post-I (BötC)	drive(RTN) {0.05} *; drive(pons) {1.65} *; early-I(1) {−0.025} *; aug-E {−0.01}; 2° Baro P){0.075} *.
post-I(e) (BötC)	drive(RTN) {0.05} *; drive(pons) {1.65} *; early-I(1) {−0.025} *; aug-E {−0.01}; P-cells {0.075}. 2° Baro {0.05} *.
CVLM * (VLM)	2° Baro {0.05} *.
RVLM * (VLM)	drive(RTN) {1} *; early-I(2){−0.01} *; post-I{−0.05} *; CVLM{−0.025} *;

Target population (location)	Excitatory drive {weight of synaptic input} or source population {weight of synaptic input from single neuron}
	IE{0.05} *.
IE * (PONS) 2° Baro P) * NTS)	ramp-I {0.2} *; post-I {0.35} *. stim *# {1}; early-I(2) {−0.05} *.
2° Baro * (NTS)	stim *# {1}.

Values in brackets represent relative weights of synaptic inputs from the corresponding source populations w_{ji} or drives w_{dmi}.

*Populations not present in the model of Smith et al. (2007) and weights of connections adjusted in the present model relative to that model.

#Stimulus representing the perfusion pressure changes PP is modelled as an integrated rectangular impulse barostimulus 400ms long of unity height with integration time constants 500ms up and 2000ms down.

References

Baekey DM, Dick TE, Paton JFR. Pontomedullary transection attenuates central respiratory modulation of sympathetic discharge, heart rate and the baroreceptor reflex in the in situ rat preparation. Exp. Physiol. 2008; 93:803–816. [PubMed: 18344259]

Barman SM, Gebber GL. Sympathetic nerve rhythm of brain stem origin. Am. J. Physiol. Regul. Integr. Comp. Physiol. 1980; 239:R42–R47.

Bianchi AL, Denavitsaubie M, Champagnant J. Central control of breathing in mammals: neuronal circuitry, membrane properties, and neurotransmitters. Physiol. Rev. 1995; 75:1–45. [PubMed: 7831394]

Bisset GS 3rd, Gaum W, Kaplan S. The ice bag: a new technique for interruption of supraventricular tachycardia. J. Pediatr. 1980; 97:593–595. [PubMed: 7420222]

Brunner MJ, Sussman MS, Greene AS, Kallman CH, Shoukas AA. Carotid sinus baroreceptor reflex control of respiration. Circ. Res. 1982; 51:624–636. [PubMed: 7139881]

Cohen MI. Neurogenesis of respiratory rhythm in the mammal. Physiol. Rev. 1979; 59:1105–1173. [PubMed: 227004]

Cohen MI, Wang SC. Respiratory neuronal activity in pons of cat. J. Neurophysiol. 1959; 22:33–50. [PubMed: 13621254]

Daly, MdB, editor. Edinburgh: Churchill Livingstone; 1984. Recent Advances in Physiology.

Daly, MdB. Interactions between respiration and circulation. In: Cherniack, NS.; Widdicombe, JG., editors. Handbook of Physiology, Section3:The Respiratory System, Volume II: Control of Breathing, part 2. Vol. vol. II. Bethesda, MD: American Physiological Society; 1986. p. 529-594.

Dampney RA. Functional organization of central pathways regulating the cardiovascular system. Physiol. Rev. 1994; 74:323–364. [PubMed: 8171117]

Dick TE, Baekey DM, Paton JFR, Lindsey BG, Morris KF. Cardio-respiratory coupling depends on the pons. Respir. Physiol. Neurobiol. 2009; 168:76–85. [PubMed: 19643216]

Dick TE, Bellingham MC, Richter DW. Pontine respiratory neurons in anesthetized cats. Brain Res. 1994; 636:259–269. [PubMed: 8012810]

Dick TE, Morris KF. Quantitative analysis of cardiovascular modulation in respiratory neural activity. J. Physiol. 2004; 556:959–970. [PubMed: 14978205]

Dick TE, Shannon R, Lindsey BG, Nuding SC, Segers LS, Baekey DM, Morris KF. Arterial pulse modulated activity is expressed in respiratory neural output. J. Appl. Physiol. 2005; 99:691–698. [PubMed: 15761086]

Dutschmann M, Herbert H. The Kölliker–Fuse nucleus gates the postinspi-ratory phase of the respiratory cycle to control inspiratory off-switch and upper airway resistance in rat. Eur. J. Neurosci. 2006; 24:1071–1084. [PubMed: 16930433]

Dutschmann M, Paton JFR. Influence of nasotrigeminal afferents on medullary respiratory neurones and the upper airway in the rat. Eur. J. Physiol. 2002; 444:227–235.

Dove EL, Katona PG. Respiratory effects of brief baroreceptor stimuli in the anesthetized dog. J. Appl. Physiol. 1985; 59:1258–1265. [PubMed: 4055605]

Elsner R, Franklin DL, Van Citters RL, Kenney DW. Cardiovascular defense against asphyxia. Science. 1966a; 153:941–949. [PubMed: 5917556]

Elsner R, Kenney DW, Burgess K. Diving bradycardia in the trained dol-phin. Nature. 1966b; 212:407–408. [PubMed: 5970155]

Ezure K. Synaptic connections between medullary respiratory neurons and considerations on the genesis of respiratory rhythm. Prog. Neurobiol. 1990; 35:429–450. [PubMed: 2175923]

Ezure K, Tanaka I, Saito Y. Brainstem and spinal projections of augmenting expiratory neurons in the rat. Neurosci. Res. 2003; 45:41–51. [PubMed: 12507723]

Ezure K, Tanaka I. Distribution and medullary projection of respiratory neurons in the dorsolateral pons of the rat. Neuroscience. 2006; 141:1011–1023. [PubMed: 16725272]

Felder RB, Mifflin SW. Modulation of carotid sinus afferent input to nucleus tractus solitarius by parabrachial nucleus stimulation. Circ. Res. 1988; 63:35–49. [PubMed: 3383382]

Feldman JL, Cohen MI. Relation between expiratory duration and rostral medullary expiratory neuronal discharge. Brain Res. 1978; 141:172–178. [PubMed: 624073]

Feldman JL, Del Negro CA. Looking for inspiration: new perspectives on respiratory rhythm. Nat. Rev. Neurosci. 2006; 7:232–242. [PubMed: 16495944]

Grunstein MM, Derenne JP, Milic-Emili J. Control of depth and frequency of breathing during baroreceptor stimulation in cats. J. Appl. Physiol. 1975; 39:395–404. [PubMed: 126222]

Guyenet, PG. Role of ventral medulla oblongata in blood pressure regulation. In: Loewy, AD.; Spyer, KM., editors. Central Regulation of Autonomic Function. Oxford, New York: Oxford University Press; 1990. p. 145-167.

Guyenet PG. Neural structures that mediate sympathoexcitation during hypoxia. Respir. Physiol. 2000; 121:147–162. [PubMed: 10963771]

Guyenet PG, Koshiya N. Working model of the sympathetic chemoreflex in rats. Clin. Exp. Hypertens. 1995; 17:167–179. [PubMed: 7735267]

Häbler H-J, Jänig W, Michaelis M. Respiratory modulation in the activity of sympathetic neurones. Prog. Neurobiol. 1994; 43:567–606. [PubMed: 7816936]

Haselton JR, Guyenet PG. Central respiratory modulation of medullary sympathoexcitatory neurons in rat. Am. J. Physiol. Regul. Integr. Comp. Physiol. 1989; 256:R739–R750.

Hayano J, Yasuma F, Okada A, Mukai S, Fujinami T. Respiratory sinus arrhythmia. A phenomenon improving pulmonary gas exchange and circulatory efficiency. Circulation. 1996; 94:842–847. [PubMed: 8772709]

Hayashi F, Coles SK, McCrimmon DR. Respiratory neurons mediating the Breuer–Hering reflex prolongation of expiration in rat. J. Neurosci. 1996; 16:6526–6536. [PubMed: 8815930]

Jiang C, Lipski J. Extensive monosynaptic inhibition of ventral respiratory group neurons by augmenting neurons in the Bötzinger Complex in the cat. Exp. Brain Res. 1990; 81:639–648. [PubMed: 2226695]

Kanjhan R, Lipski J, Kruszewska B, Rong W. A comparative study of pre-sympathetic and Bötzinger neurons in the rostral ventrolateral medulla (RVLM) of the rat. Brain Res. 1995; 699:19–32. [PubMed: 8616610]

Koepchen HP, Klüssendorf D, Sommer D. Neurophysiological background of central neural cardiovascular–respiratory coordination: basic remarks and experimental approach. J. Auton. Nerv. Syst. 1981; 3:335–368. [PubMed: 6792255]

Koshiya N, Guyenet PG. Tonic sympathetic chemoreflex after blockade of respiratory rhythmogenesis in the rat. J. Physiol. 1996; 491:859–869. [PubMed: 8815217]

Koshiya N, Smith JC. Neuronal pacemaker for breathing visualized in vitro. Nature. 1999; 400:360–363. [PubMed: 10432113]

Krolo M, Tonkovic-Capin V, Stucke AG, Stuth EA, Hopp FA, Dean C, Zuperku EJ. Subtype composition and responses of respiratory neurons in the pre-botzinger region to pulmonary afferent inputs in dogs. J. Neurophysiol. 2005; 93:2674–2687. [PubMed: 15601729]

Li Z, Morris KF, Baekey DM, Shannon R, Lindsey BG. Responses of simultaneously recorded respiratory-related medullary neurons to stimulation of multiple sensory modalities. J. Neurophysiol. 1999a; 82:176–187. [PubMed: 10400946]

Li Z, Morris KF, Baekey DM, Shannon R, Lindsey BG. Multimodal medullary neurons and correlational linkages of the respiratory network. J. Neurophysiol. 1999b; 82:188–201. [PubMed: 10400947]

Lindsey BG, Arata A, Morris KF, Hernandez YM, Shannon R. Medullary raphe neurones and baroreceptor modulation of the respiratory motor pattern in the cat. J. Physiol. 1998; 512:863–882. [PubMed: 9769428]

Loewy, AD.; Spyer, KM., editors. Central regulation of autonomic functions. New York: Oxford University Press; 1990.

Lumsden T. Observations on the respiratory centres in the cat. J. Physiol. 1923; 57:153–160. [PubMed: 16993609]

Manabe M, Ezure K. Decrementing expiratory neurons of the BötzingerCom-plex. I. Response to lung inflation and axonal projection. Exp. Brain Res. 1988; 72:150–158. [PubMed: 3169182]

Mandel DA, Schreihofer AM. Central respiratory modulation of barosensi-tive neurones in rat caudal ventrolateral medulla. J. Physiol. 2006; 572:881–896. [PubMed: 16527859]

Mandel DA, Schreihofer AM. Modulation of the sympathetic response to acute hypoxia by the caudal ventrolateral medulla in rats. J. Physiol. 2009; 587:461–475. [PubMed: 19047207]

McMullan S, Dick TE, Farnham MM, Pilowsky PM. Effects of baroreceptor activation on respiratory variability in rat. Respir. Physiol. Neurobiol. 2009; 166(2):80–86. [PubMed: 19429523]

Miyazaki M, Tanaka I, Ezure K. Excitatory and inhibitory synaptic inputs shape the discharge pattern of pump neurons of the nucleus tractus solitarii in the rat. Exp. Brain Res. 1999; 129:191–200. [PubMed: 10591893]

Morrison SF. Respiratory modulation of sympathetic nerve activity: effect of MK-801. Am. J. Physiol. 1996; 270:R645–R651. [PubMed: 8780232]

Nishino T, Honda Y. Changes in pattern of breathing following baroreceptor stimulation in cats. Jpn. J. Physiol. 1982; 32:183–195. [PubMed: 6809994]

Parkes MJ, Lara-Munoz JP, Izzo PN, Spyer KM. Responses of ventral respiratory neurones in the rat to vagus stimulation and the functional division of expiration. J. Physiol. 1994; 476:131–139. [PubMed: 8046628]

Paton JF. A working heart-brainstem preparation of the mouse. J. Neurosci. Methods. 1996; 65:63–68. [PubMed: 8815310]

Paxinos, G.; Watson, C. The Rat Brain in Stereotaxic Coordinates. fourth ed. New York: Academic Press; 1998.

Pilowsky PM, Jiang C, Lipski J. An intracellular study of respiratory neurons in the rostral ventrolateral medulla of the rat and their relationship to catecholamine-containing neurons. J. Comp. Neurol. 1990; 301:604–617. [PubMed: 1980279]

Pilowsky P, Llewellyn-Smith IJ, Lipski J, Minson J, Arnolda L, Chalmers J. Projections from inspiratory neurons of the ventral respiratory group to the subretrofacial nucleus of the cat. Brain Res. 1994; 633:63–71. [PubMed: 7907937]

Pilowsky P, Wakefield B, Minson J, Llewellyn-Smith I, Chalmers J. Axonal projections from respiratory centres towards the rostral ventrolateral medulla in the rat. Clin. Exp. Pharmacol. Physiol. 1992; 19:335–338. [PubMed: 1521365]

Potter EK. Inspiratory inhibition of vagal responses to baroreceptor and chemoreceptor stimuli in the dog. J. Physiol. 1981; 316:177–190. [PubMed: 7320863]

Rekling JC, Feldman JL. PreBötzinger Complex and pacemaker neurons: hypothesized site and kernel for respiratory rhythm generation. Annu. Rev. Physiol. 1998; 60:385–405. [PubMed: 9558470]

Richter, DW. Neural regulation of respiration: rhythmogenesis and afferent control. In: Greger, R.; Windhorst, U., editors. Comprehensive Human Physiology. Berlin: Springer-Verlag; 1996. p. 2079-2095.

Richter DW, Seller H. Baroreceptor effects on medullary respiratory neurones of the cat. Brain Res. 1975; 86:168–171. [PubMed: 163666]

Richter, DW.; Spyer, KM. Cardiorespiratory control. In: Loewy, AD.; Spyer, KM., editors. Central Regulation of Autonomic function. Oxford, New York: Oxford University Press; 1990. p. 189-207.

Richter DW, Spyer KM. Studying rhythmogenesis of breathing: comparison of in vivo and in vitro models. Trends Neurosci. 2001; 24:464–472. [PubMed: 11476886]

Rogers RF, Paton JF, Schwaber JS. NTS neuronal responses to arterial pressure and pressure changes in the rat. Am. J. Physiol. 1993; 265:R1355–R1368. [PubMed: 8285278]

Rybak IA, Shevtsova NA, Paton JF, Dick TE, St-John WM, Mörschel M, Dutschmann M. Modeling the ponto-medullary respiratory network. Respir. Physiol. Neurobiol. 2004; 143:307–319. [PubMed: 15519563]

Rybak IA, Abdala AP, Markin SN, Paton JF, Smith JC. Spatial organization and state-dependent mechanisms for respiratory rhythm and pattern generation. Prog. Brain Res. 2007; 165:201–220. [PubMed: 17925248]

Rybak IA, O'Connor R, Ross A, Shevtsova NA, Nuding SC, Segers LS, Shannon R, Dick TE, Dunin-Barkowski WL, Orem JM, Solomon IC, Morris KF, Lind-sey BG. Reconfiguration of the pontomedullary respiratory network: a computational modeling study with coordinated in vivo experiments. J. Neurophysiol. 2008; 100:1770–1799. [PubMed: 18650310]

Segers LS, Nuding SC, Dick TE, Shannon R, Baekey DM, Solomon IC, Morris KF, Lindsey BG. Functional connectivity in the pontomedullary respiratory network. J. Neurophysiol. 2008; 100:1749–1769. [PubMed: 18632881]

Simms AE, Paton JF, Pickering AE. Hierarchical recruitment of the sympathetic and parasympathetic limbs of the baroreflex in normotensive and spontaneously hypertensive rats. J. Physiol. 2007; 579:473–486. [PubMed: 17170043]

Simms AE, Paton JF, Pickering AE, Allen AM. Amplified respiratory– sympathetic coupling in the spontaneously hypertensive rat: does it contribute to hypertension? Auton. Neurosci. 2009; 142:32–39. [PubMed: 18479978]

Simms AE, Paton JFR, Pickering AE, Allen AM. Is augmented central respiratory–sympathetic coupling involved in the generation of hypertension? Respir. Physiol. Neurobiol. 2010 Epub ahead of print.

Smith JC, Ellenberger HH, Ballanyi K, Richter DW, Feldman JL. Pre-Bötzinger Complex: a brainstem region that may generate respiratory rhythm in mammals. Science. 1991; 254:726–729. [PubMed: 1683005]

Smith JC, Abdala AP, Koizumi H, Rybak IA, Paton JF. Spatial and functional architecture of the mammalian brain stem respiratory network: a hierarchy of three oscillatory mechanisms. J. Neurophysiol. 2007; 98:3370–3387. [PubMed: 17913982]

Smith JC, Abdala AP, Rybak IA, Paton JF. Structural and functional architecture of respiratory networks in the mammalian brainstem. Philos. Trans. R. Soc. Lond. B. Biol. Sci. 2009; 364:2577–2587. [PubMed: 19651658]

Speck DF, Webber CL Jr. Baroreceptor modulation of inspiratory termination by intercostal nerve stimulation. Respir. Physiol. 1983; 52:387–395. [PubMed: 6612108]

Stella MH, Knuth SL, Bartlett D. Respiratory response to baroreceptor stimulation and spontaneous contractions of the urinary bladder. Respir. Physiol. 2001; 124:169–178. [PubMed: 11173072]

Sun QJ, Minson J, Llewellyn-Smith IJ, Arnolda L, Chalmers J, Pilowsky P. Bötzinger neurones project towards bulbospinal neurones in the rostral ventro-lateral medulla of the rat. J. Comp. Neurol. 1997; 388:23–31. [PubMed: 9364236]

Takagi K, Nakayama T. Respiratory discharge of the pons. Science. 1958; 128:1206. [PubMed: 13592305]

Tian GF, Peever JH, Duffin J. Bötzinger-Complex, bulbospinal expiratory neurones monosynaptically inhibit ventral-group respiratory neurones in the decerebrate rat. Exp. Brain Res. 1999; 124:173–180. [PubMed: 9928840]

Whayne TF Jr, Killip T 3rd. Simulated diving in man: comparison of facial stimuli and response in arrhythmia. J. Appl. Physiol. 1967; 22:800–807. [PubMed: 6023194]

Wildenthal K, Leshin SJ, Atkins JM, Skelton CL. The diving reflex used to treat paroxysmal atrial tachycardia. Lancet. 1975; 1:12–14. [PubMed: 46336]

Zoccal DB, Paton JF, Machado BH. Do changes in the coupling between respiratory and sympathetic activities contribute to neurogenic hypertension? Clin. Exp. Pharmacol. Physiol. 2009; 36:1188–1196. [PubMed: 19413588]

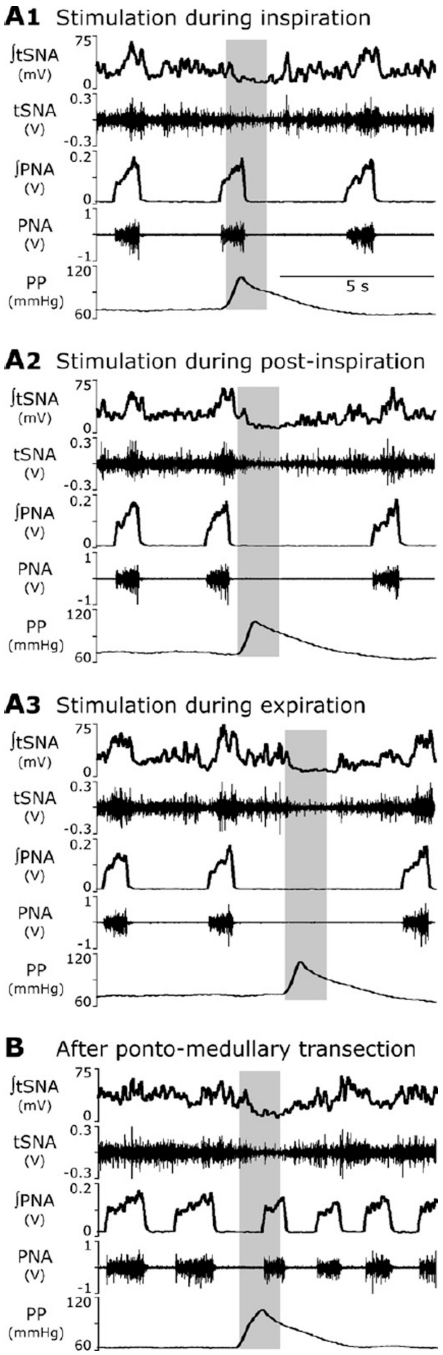

Fig. 1.

Response of the sympathetic (SNA, top pair of traces) and phrenic (PNA, middle pair of traces) nerve activities to transient increases in perfusion pressure (PP, bottom trace). (A1–A3) Stimulation was applied to the intact preparation during inspiration (A1), post-inspiration (A2) and late expiration (A3). Note that the stimulus applied during inspiration did not affect the respiratory pattern (A1), whereas the stimuli delivered during the expiratory phase prolonged expiration (A2, A3). This T_E prolongation was stronger when stimulus was applied later in expiration. (B) The effect of baroreceptor stimulation after pontine transection. The applied stimulus did not prolong expiration, but shortened the

apneustic inspiratory PNA bursts. Traces from top to bottom: integrated and raw SNA, integrated and raw PNA, and perfusion pressure are shown on each panel.

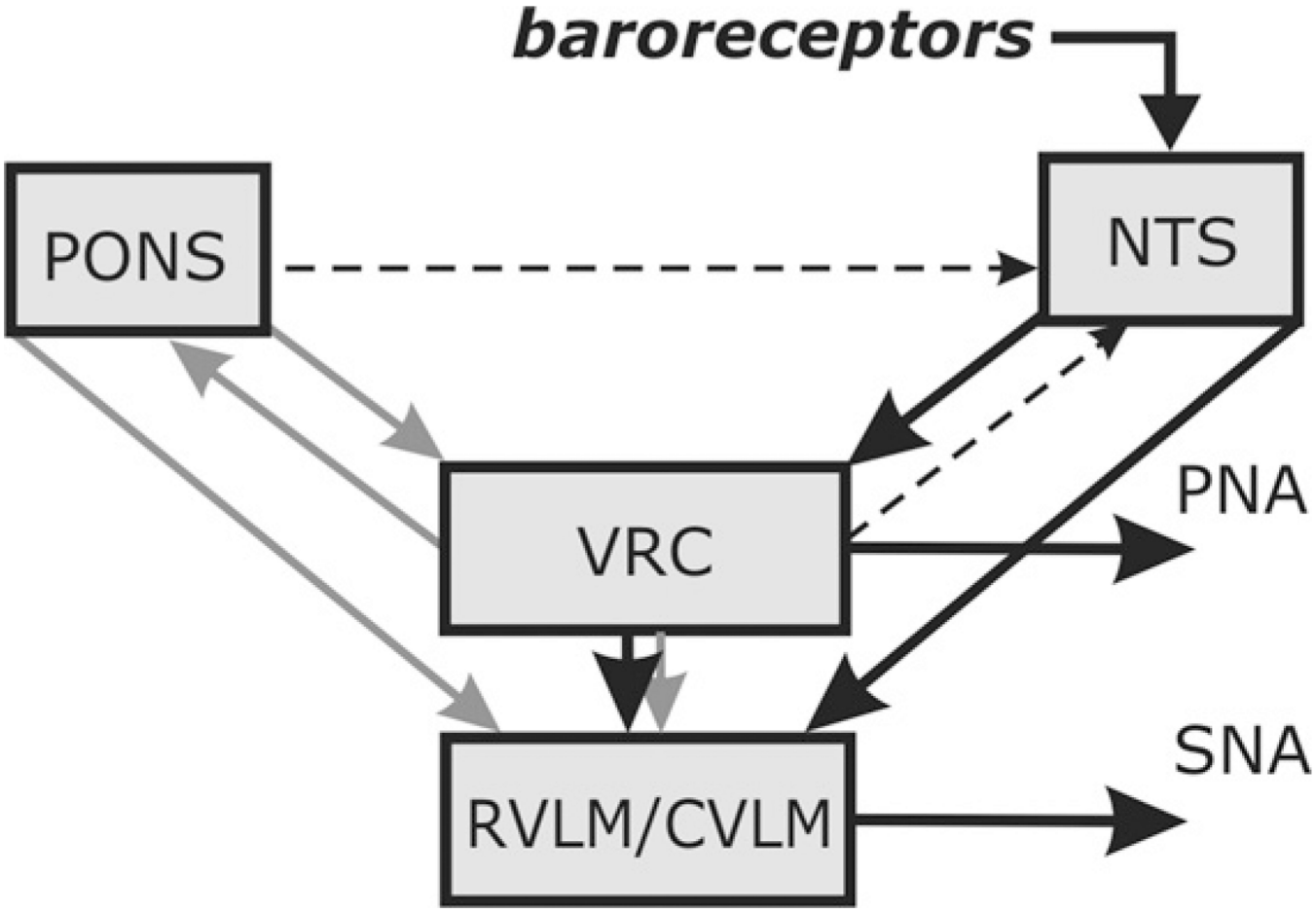

Fig. 2.

Conceptual model of interaction among respiratory-related activity of the ventral respiratory column (VRC), pontine circuits (PONS), sensory network in the nucleus tractus solitarii (NTS) and rostral and caudal ventrolateral medulla (RVLM/CVLM). The sympathetic baroreceptor reflex operates via two pathways (thick line, large arrows): one direct pathway includes baroreceptors, NTS baro-sensitive cells and CVLM, which inhibits RVLM and SNA; the other indirect pathway goes from baroreceptors through NTS and VRC, whose post-inspiratory neurones inhibit RVLM and SNA. Grey arrows represent the effects of VRC and PONS on RVLM providing respiratory modulation of SNA. Another grey arrow indicates the effects of VRC on PONS providing respiratory modulation of pontine neurones. Finally, two dashed arrows indicate central suppression of the baroreflex gain during inspiration which potentially can be provided by VRC or pontine neurones see details in the text).

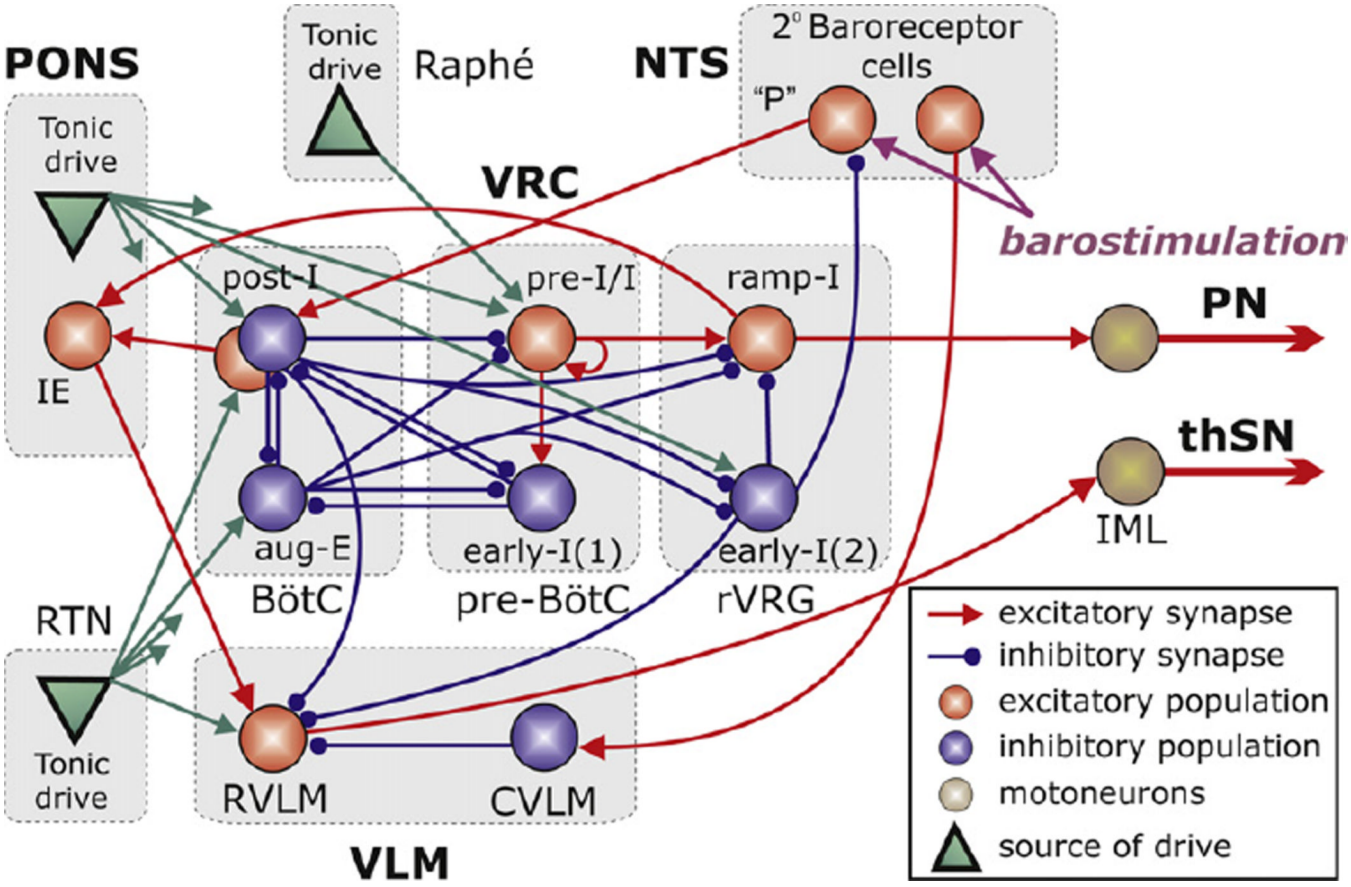

Fig. 3.

The schematic of the extended computational model showing interactions between different populations of respiratory neurones within major brainstem compartments involved in the control of breathing and sympathetic motor activity pons, RTN, BötC, pre-BötC, rVRG, VLM, Raphé, and NTS). A 'sphere' represents each population, which consists of 20–50 single-compartment neurones described in the Hodgkin–Huxley style. In comparison with the previous model (Smith et al., 2007), this model additionally incorporates RVLM and CVLM populations in the VLM, an IE phase-spanning population in the pons, and two populations of barosensitive cells in the NTS. The model includes three sources of tonic excitatory drive located in the pons, RTN and raphé shown as green triangles. These drives, especially those from the pontine and RTN sources project to multiple neural populations in the model (green arrows). However,to simplify the schematic, only the most important connections are shown connected to particular populations. The full structure of connections from each drive source (pons/RTN/raphé) to target neural populations of the model and the corresponding synaptic weights are in Table 1 in the Appendix.

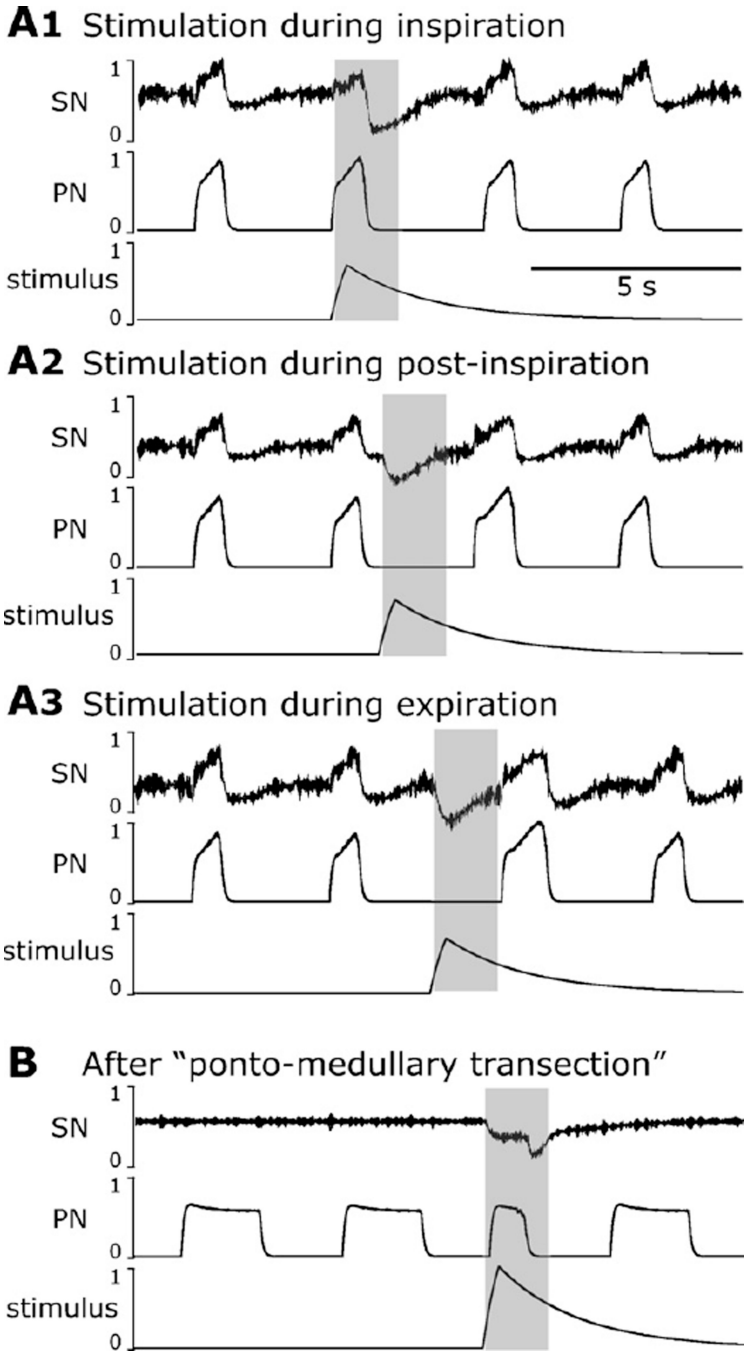

Fig. 4.

Simulations of the effect of phase-dependent barostimulation on the phrenic (PN) and sympathetic (SN) nerve outputs. Stimulus was applied during inspiration (A1), post-inspiration (A2) and late expiration (A3). In A1, the stimulus applied during inspiration had no effect on respiratory phase durations; SN activity during stimulation is attenuated due to baroreflex. In (A2, A3), the stimuli during expiration prolonged expiration, slightly when applied in post-inspiration or substantially, in late expiration. (B) After removal of the pontine compartment in the model, the applied stimulation does not prolong the expiratory period, but shorten the "apneustic" PN bursts if applied during inspiration. SN activity

respiratory modulation is abolished. Traces are as Fig. 1. The phases of barostimulation are chosen approximately the same as in experimental examples in Fig. 1.

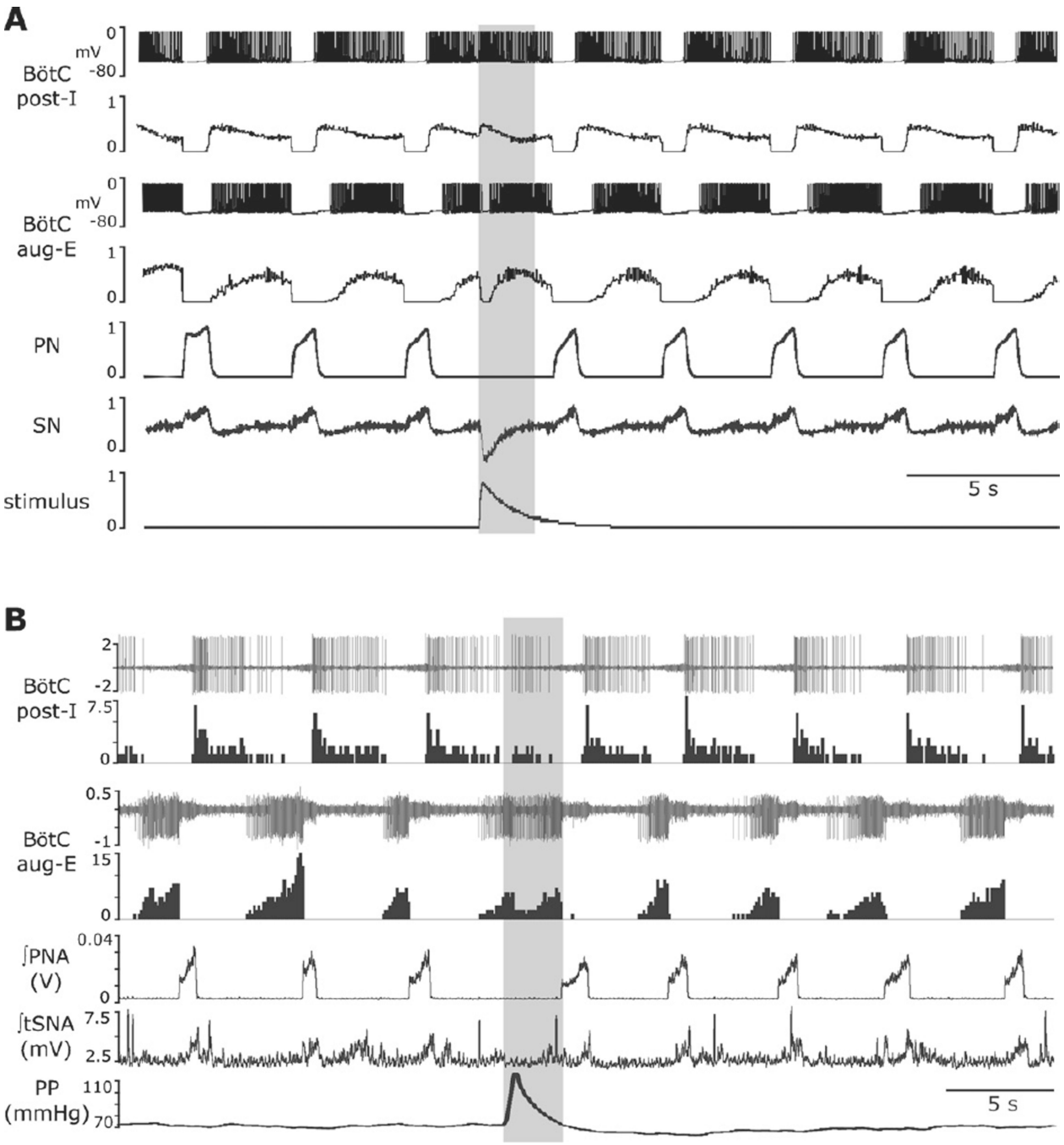

Fig. 5.

Response to transient baroreceptor stimulation in the model and in situ. (A) Simulation results. The top pair of traces: membrane potential of a randomly chosen neurone from the post-I population of BötC and integrated spike histogram of the entire post-I population. Second pair of traces: membrane potential of a randomly chosen neurone from the aug-E population of BötC and spike histogram of the entire aug-E population. The applied stimulation (lowest trace) excited post-I neurones and inhibited aug-E neurones. After the stimulus ended, the aug-E neuroneactivated again. The transient changes in post-I and aug-E activities prolonged expiration. (B) Experimental results in situ preparation: the applied baro-stimulus activated post-I and suppressed aug-E activities. These changes in neurone

activity were associated with decreased SNA output and prolongation of expiration. Traces in (B): top two traces show an extracellular recording from a post-I neurone in BötC and the histogram of its activity; the next pair of traces show a simultaneous extracellular recording from an aug-E neurone of BötC and the corresponding histogram; the remaining traces show the integrated phrenic nerve activity (PNA), integrated thoracic sympathetic nerve activity (tSNA), and perfusion pressure (PP). The response to the applied barostimulation in the in situ preparation is associated with increases in post-I and decreases in aug-E activity and prolongation of the expiratory phase. These neuronal activity patterns of the recorded post-I and aug-E neurones are consistent with the proposed connectivity between these two types of neurones located in the BötC.